Title: A PI3K-mediated negative feedback regulates Drosophila motor neuron excitability

Authors: Eric Howlett[1], Curtis Chun-Jen Lin[1], William Lavery[1] and Michael Stern[1]

Dept. of Biochemistry and Cell Biology, Rice University, Houston, Texas, 77251

Negative feedback processes, which can enable maintenance of neuronal homeostasis, are widely observed in neuronal systems[1-3]. For example, neuronal silencing via tetrodotoxin application both *in vivo* and *in vitro* increases excitability[4-6]. This effect occurs *in vitro* via both increased sodium currents and decreased potassium currents. However, the signalling pathways responsible for these excitability changes remain unclear. The mammalian type II metabotropic glutamate receptors, which are G-protein coupled receptors activated by glutamate, are well positioned to mediate negative feedback. When localized presynaptically, these receptors can act as autoinhibitors of glutamate release[7-10]. Because these receptors are located outside of the active zone[11], activation is thought to occur only during conditions of elevated glutamate release and might serve to prevent glutamate-mediated neurotoxicity. Agonists for these receptors are proposed for treatment of schizophrenia, anxiety and epilepsy, among others[12, 13], but although many of the acute effects of type II mGluR activation on neuronal physiology have been elucidated[14, 15], possible long term effects on neuronal function, such as through changes in ion channel gene expression, remain essentially unexplored.

The Drosophila mGluRA affects the rate of onset of long-term facilitation (LTF), a reporter for motor neuron excitability: In Drosophila, the single *mGluRA*

gene encodes a protein most similar to the mammalian type II mGluR[16]. mGluRA is located presynaptically at the neuromuscular junction (nmj), which suggests that mGluRA might regulate transmitter release from motor neurons. Elimination of *mGluRA* by the null mutation *mGluRA*^{112b} affects a form of synaptic plasticity termed long-term facilitation (LTF)[16, 17], which is induced when a motor neuron is subjected to repetitive nerve stimulation at low bath [Ca^{2+}]. At a certain point in the stimulus train, an abrupt increase in transmitter release and hence muscle depolarization (termed excitatory junctional potential, or ejp) is observed (Figure 1A). This abrupt increase is caused by an abrupt increase in the duration of nerve terminal depolarization and hence Ca^{2+} influx, and reflects a progressive increase in motor neuron excitability induced by the repetitive nerve stimulation: when an excitability threshold is reached, LTF occurs[17-19].

In Drosophila, many genotypes that increase motor neuron excitability by decreasing K^+ currents or increasing Na^+ currents increase the rate of onset of LTF. For example, altered activities of *frequenin* and *Hyperkinetic*, which act via K^+ channels, or *paralytic* and *pumilio*, which act via Na^+ channels, each increase the rate of onset of LTF[18-25]. By increasing motor neuron excitability, these genotypes apparently bring excitability closer to the threshold required to evoke LTF and consequently decrease the number of prior nerve stimulations required to reach this threshold. The observation that *mGluR*^{112b} increases the rate of onset of LTF suggested that *mGluR*^{112b} increases motor neuron excitability as well[16].

Glutamate-activation of mGluRA decreases neuronal excitability by preventing PI3K activation: In addition to increasing neuronal excitability, *mGluR*^{112b} also decreased arborization and synapse number at the larval neuromuscular junction[16].

This phenotype is also observed in larval motor neurons with decreased activity of PI3K[26]. This observation raised the possibility that mGluRA might exert its effects on both synapse formation and neuronal excitability via PI3K activity. To test this possibility, we used the *Gal4/UAS* system[27] to overexpress transgenes expected to alter activity of the motor neuron PI3K pathway. We found that inhibiting the PI3K pathway by motor neuron specific overexpression of either the phosphatase *PTEN*, which opposes the effect of PI3K, or the dominant-negative $PI3K^{DN}$ [28], each significantly increased the rate of onset of LTF, similarly to that of $mGluRA^{112b}$ (Figure 1A and 1B). In contrast, we found that activating the PI3K pathway by expression of the constitutively active *PI3K-CAAX* [28], or via RNAi-mediated inhibition of *PTEN* decreased rate of onset of LTF (Figure 1A and 1B). These observations support the notion that loss of mGluRA increases motor neuron excitability by preventing the activation of the PI3K pathway. A role for type II mGluRs in PI3K pathway activation, and for the PI3K pathway in the control of neuronal excitability, are each novel findings.

In addition to effects on LTF, mutations that alter motor neuron excitability can alter basal transmitter release and hence ejp amplitude at low bath Ca^{2+} concentrations, at which Ca^{2+} influx would be limiting for vesicle fusion to occur. For example, mutations in *ether-a go-go (eag)*, which encodes a potassium channel α subunit, increase transmitter release about two-fold[29], whereas a mutation in the sodium channel gene *paralytic* decreases transmitter release by increasing the frequency of failures of vesicle release[30]. Presumably altered excitability affects the amplitude or duration of the action potential and consequently the amount of Ca^{2+} influx through voltage-gated channels. We found that $mGluRA^{112b}$ also increased ejp amplitude and hence basal transmitter

release at three low bath Ca^{2+} concentrations tested (Figure 1C), which is consistent with increased motor neuron excitability in this genotype. To test if altering the PI3K pathway would similarly affect basal transmitter release, we compared ejp amplitudes in larvae with altered activity of the PI3K pathway in motor neurons. We found that decreasing PI3K pathway activity via motor neuron overexpression of *PI3K*^{DN} or *PTEN* increased transmitter release to levels similar to *mGluRA*^{112b}, whereas increasing PI3K pathway activity via overexpression of *PI3K-CAAX* decreased basal transmitter release (Figure 1C).

The *mGluRA*^{112b} mutation also decreased the frequency at which failures of vesicle release occur, particularly at the lower Ca^{2+} concentrations tested (Supplementary Figure 1B). This observation confirms that the effect of *mGluRA*^{112b} on ejp amplitude is presynaptic. We also observed a decreased frequency of failures when the PI3K pathway was inhibited by motor neuron expression of *PI3K*^{DN} or *PTEN* (Supplementary Figure 1A). In contrast, motor neuron overexpression of *PI3K-CAAX* increased the frequency of failures (Supplementary Figure 1A). Therefore, with three electrophysiological readouts, the *mGluRA*^{112b} mutant phenotype was mimicked by decreased activity of the PI3K pathway, whereas increasing PI3K pathway activity conferred opposite effects.

The effects of PI3K on neuronal excitability are mediated by Foxo, not Tor/S6 kinase: Many effects of the PI3K pathway are mediated by the downstream kinase Akt. Activated Akt phosphorylates and inhibits targets such as Tsc1/Tsc2, which regulates cell growth via the Tor/S6 Kinase (S6K) pathway[31], Foxo, which regulates apoptosis[32], and GSK3[33], which mediates at least in part the effects of altered PI3K pathway activity on arborization and synapse formation[26]. To determine if the Tor/S6K

pathway mediates the effects of altered PI3K pathway activity on neuronal excitability, we tested the effects of overexpression of either the dominant-negative *S6K*^{DN} or the constitutively active *S6K*^{Act} transgene[34] in motor neurons. We found that the rate of onset of LTF was unaffected by expression of both transgenes (Figure 1D), and that expression of *S6K*^{DN} had no effect on the ability of *PI3K-CAAX* to decrease the rate of onset of LTF (Figure 1D). Furthermore, expression of *S6K*^{DN} had no effect on basal transmitter release, and did not affect the ability of *PI3K-CAAX* to depress basal transmitter release (data not shown). Therefore we conclude that the Tor/S6K pathway does not mediate the effects of PI3K on neuronal excitability.

To determine if Foxo mediates the effects of altered PI3K pathway activity on neuronal excitability, we measured the rate of onset of LTF in larvae carrying the heteroallelic *Foxo*^{21}*/Foxo*^{25} null mutant combination[35] and in larvae overexpressing *Foxo*$^{+}$ [36] in motor neurons. We found that overexpression of *Foxo*$^{+}$ increased the rate of onset of LTF to a level very similar to that observed when PI3K pathway activity was decreased (Figure 1D), whereas in *Foxo*^{21}*/Foxo*^{25} larvae, both the rate of onset of LTF and basal transmitter release were decreased, and the frequency of failures increased, to levels very similar to those observed when PI3K pathway activity was increased (Figure 1C, Figure 1D and Supplementary Figure 1B). These results are consistent with the possibility that the effects of increased PI3K activity on neuronal excitability are mediated entirely by Foxo inhibition.

The effects of PI3K on synapse formation are mediated by Tor/S6 kinase, not Foxo: Because altered PI3K pathway activity alters motor neuron arborization and synapse formation[26], it seemed possible that a causal relationship existed between the

PI3K-mediated excitability and neuroanatomy defects. To test this possibility, we evaluated the roles of the Tor/S6K and Foxo pathways in mediating the effects of altered PI3K activity on synapse formation. We found that motor neuron-specific expression of $S6K^{Act}$ increased bouton number to an extent similar to *PI3K-CAAX*, and motor neuron expression of $S6K^{DN}$ decreased bouton number to the same extent as $PI3K^{DN}$ while also partially suppressing the increase in bouton number conferred by *PI3K-CAAX* (Supplementary Figure 2). This partial suppression suggests that both Tor/S6K and a second, PI3K-mediated, pathway (presumably involving GSK3) regulate synapse formation. In contrast to the effects of altered S6K on synapse formation, we found that $Foxo^{+}$ overexpression had no effect on synapse number (data not shown) and failed to suppress the growth-promoting effects of PI3K-CAAX (Supplementary Figure 2).

The PI3K pathway also affects growth along the length of axons and thus regulates axon diameter. In Drosophila peripheral nerves, about 80 motor and sensory axons are wrapped by about three layers of glia, as shown in the transmission electron micrograph from cross sections of peripheral nerves in Supplementary Figure 2C. We found that motor neuron specific expression of *PTEN* decreased axon diameter, whereas motor-neuron specific expression of *PI3K-CAAX* increased axon diameter. Tor/S6K, but not Foxo, mediates this growth effect. In particular, motor neuron-specific expression of $S6K^{Act}$ increased axon diameter to an extent similar to *PI3K-CAAX*, and motor-neuron-specific expression of $S6K^{DN}$ decreased motor axon diameter to an extent similar to *PTEN* and also partially suppressed the growth-promoting effects conferred by *PI3K-CAAX*. In contrast, $Foxo^{+}$ overexpression had no effect on the ability of PI3K-CAAX to increase axon diameter (Supplementary Figure 2D). Therefore, Foxo mediates the

excitability effects, but not the growth-promoting effects, of altered PI3K pathway activity. We conclude that the excitability and growth effects are completely separable genetically and thus have no causal relationship.

Epistasis tests among mGluRA, PI3K and Foxo support a model for the glutamate-induced negative feedback regulation of neuronal excitability: The effects on neuronal excitability of altered mGluRA, PI3K, and Foxo activities are consistent with a model in which glutamate released from motor nerve terminals as a consequence of motor neuron activity activates motor neuron PI3K via mGluRA autoreceptors, which then downregulate neuronal excitability via inhibition of Foxo (Figure 2). Foxo, in turn, might regulate excitability via transcription of ion channel subunits or regulators. This model predicts the outcomes of several epistasis tests. First, the hyperexcitability of $mGluRA^{112b}$ is predicted to result from low PI3K activity. If so, then motor neuron expression of *PI3K-CAAX* will suppress this hyperexcitability. We found that larvae expressing *PI3K-CAAX* in an $mGluRA^{112b}$ background exhibited a rate of onset of LTF, basal transmitter release, and failure frequency very similar to what was observed when *PI3K-CAAX* was expressed in a wildtype background (Supplementary Figure 1 and Supplementary Figure 3). Second, the hyperexcitability conferred by motor neuron expression of $PI3K^{DN}$ is predicted to result from $Foxo^{+}$ hyperactivity. If so, then the absence of Foxo protein will suppress this hyperexcitability. We found that larvae carrying the $Foxo^{21}/Foxo^{25}$ null combination and expressing $PI3K^{DN}$ in motor neurons exhibited a rate of onset of LTF, basal transmitter release, and failure frequency very similar to what was observed in the $Foxo^{21}/Foxo^{25}$ null mutant alone (Figure 3 and Supplementary Figure 1). Third, the hypoexcitability conferred by motor neuron

expression of *PI3K-CAAX* is predicted to result from decreased Foxo activity. If so, then $Foxo^{+}$ overexpression will suppress this hypoexcitability. We found that larvae co-expressing $Foxo^{+}$ and *PI3K-CAAX* in motor neurons exhibited basal transmitter release and failure frequency very similar to what was observed when $PI3K^{DN}$ or *PTEN* alone were expressed in motor neurons (Figure 3 and Supplementary Figure 1), and the rate of onset of LTF was very similar to what was observed when $Foxo^{+}$ alone was expressed in motor neurons (Figure 1D and Figure 3). Fourth, the hyperexcitability conferred by $mGluRA^{112b}$ is predicted to result from Foxo hyperactivity. If so, then the absence of Foxo protein will suppress this hyperexcitability. We found that basal transmitter release and failure frequency in $Foxo^{21}/Foxo^{25}$; $mGluRA^{112b}$ larvae were very similar to what was observed in $Foxo^{21}/Foxo^{25}$; $mGluRA^{+}$ (Supplementary figure 1 and Supplementary Figure 3) and rate of onset of LTF was also significantly, but partially, suppressed (Supplementary figure 3). This observation supports the notion that glutamate-activation of mGluRA decreases neuronal excitability by decreasing $Foxo^{+}$ activity, but the ability of $Foxo^{21}/Foxo^{25}$ to suppress the $mGluRA^{112b}$ LTF phenotype only partially raises the possibility that mGluRA might also regulate neuronal excitability in a Foxo-independent manner. The model shown in Figure 2 is strongly supported by the ability of the model to predict successfully the results of these epistasis tests.

Glutamate application increases motor nerve terminal phospho-Akt levels in an mGluRA-dependent fashion: Next we wanted to test directly the prediction that glutamate activates PI3K via mGluRA autoreceptors within motor neurons. To assay for PI3K activity, we applied an antibody specific for the phosphorylated form of Akt (p-Akt), which is increased by elevated PI3K pathway activity. The ability to detect p-Akt

in larval motor neurons overexpressing *PI3K-CAAX*, but not in wildtype (Figure 4), validates this antibody as a PI3K reporter.

To determine if glutamate application would activate PI3K in motor nerve terminals, we compared p-Akt levels in wildtype versus $mGluRA^{112b}$ motor nerve terminals immediately prior to or following a 1 minute application of 100 µM glutamate. We found that glutamate application strongly increased p-Akt levels in wildtype larvae, but not in the $mGluRA^{112b}$ larvae (Figure 4), demonstrating that glutamate application increases nerve terminal p-Akt levels, and that mGluRA activity is required for this increase. To determine if mGluRA activity was required presynaptically for this p-Akt increase, we knocked down mGluRA levels specifically in the motor neuron via motor neuron-specific expression of an *mGluRA* RNAi construct, which was previously shown to decrease mGluRA levels successfully[16]. We found that motor neuron specific knockdown of *mGluRA*, or motor neuron-specific expression of $PI3K^{DN}$, significantly inhibited the ability of glutamate to increase p-Akt levels (Figure 4). Thus, presynaptic mGluRA and PI3K activity are both necessary for glutamate to increase p-Akt.

Activity-dependent increase in synapse formation requires PI3K activity: Depending on the system, neuronal activity can either restrict or promote synapse formation[37]. The Drosophila *eag Sh* double mutant, in which two distinct potassium channel subunits are simultaneously disrupted, displays extreme neuronal hyperexcitability[29], and a consequent increase in synapse number[38]. This activity-dependent increase in synapse formation does not require mGluRA activity[16], suggesting that excessive glutamate release is not necessary for this excessive growth to occur. To determine if PI3K activity is required for this overgrowth, we compared synapse number

in wildtype larvae, in larvae expressing dominant-negative transgenes for both *eag* (*eag*^{DN}) and *Sh* (*Sh*^{DN})[39, 40] in motor neurons, and in larvae co-expressing *eag*^{DN}, *Sh*^{DN} and *PI3K*^{DN}. We found that co-expression of *eag*^{DN} and *Sh*^{DN} in motor neurons increased synapse number similarly to what was observed previously[38], and that this increase was completely blocked by simultaneous expression of *PI3K*^{DN} but not by *lacZ* (Figure 5). Thus, the activity-dependent increase in synapse formation requires PI3K activity. The observation that glutamate activation of mGluRA is not necessary for this increase raises the possibility that another PI3K activator contributes to synapse formation at the larval nmj. Insulin is a plausible candidate for such an activator because both insulin and insulin receptor immunoreactivity are present at the nmj[41].

Other negative feedback systems at the Drosophila nmj: The mGluRA-dependent negative feedback reported here co-exists with several other negative feedback systems operating at the Drosophila nmj. In addition to altered excitability, these systems include alterations in the vesicle release properties of the motor nerve terminal and density of the muscle glutamate receptors[1]. Presumably, these diverse feedback systems regulate specific aspects of neuronal function. For example, the mGluRA-dependent feedback system reported here might protect neurons from excitotoxic effects of prolonged stimulation; such protection would not be accomplished by the other feedback systems operating. In addition, because the mGluRA-dependent feedback apparently involves transcriptional changes, the system is expected to operate on a long time scale (minutes to hours) and thus be responsive to chronic, rather than acute, changes in neuronal activity.

Neuronal excitability in human disease: Human orthologues of the molecules described here are implicated in several neurological disorders. For example, type II mGluRs are potential drug targets for schizophrenia, epilepsy, and anxiety disorders[12-14], raising the possibility that altered excitability of glutamatergic neurons might play a role in these disorders. In addition, levels of phospho-Foxo, a product of PI3K/Akt activity, are increased following induction of seizures in rats, and in the hippocampi of epileptic patients[42]. This activity-induced increase in phospho-Foxo was interpreted as a mechanism to protect neurons from the excitotoxic effects of excessive glutamate release because Foxo, but not phospho-Foxo, can promote apoptosis. Our results raise the possibility that this increased phospho-Foxo occurs via glutamate-induced PI3K activation mediated by type II mGluRs, and interpret this increase as a negative feedback on excitability. These interpretations are not mutually exclusive. Increased insulin/IGF levels and increased PI3K activity are also implicated in autism spectrum disorders[43, 44]. These increases are generally hypothesized to affect neuronal function by increasing arborization and synapse formation, but our results raise the possibility that altered neuronal excitability might also contribute. Finally, increased PI3K activity is implicated in nervous system tumors occurring in individuals with the genetic disorder type 1 Neurofibromatosis[45-47]. Our results raise the possibility that learning disabilities associated with this disease might involve PI3K-dependent alterations in neuronal excitability. Thus, the results reported here might have significance for several human neurological disorders.

A novel signalling pathway linking type II mGluRs and PI3K: The mechanism by which glutamate-activated mGluRA activates PI3K remains unknown.

Although mammalian type I mGluRs activate PI3K via the Homer scaffolding protein and the PI3K enhancer PIKE[48], Drosophila mGluRA, similar to mammalian type II mGluRs, lack Homer binding motifs[49] and thus would not be predicted to activate PI3K by this mechanism. Alternatively, although the inhibition of glutamate-induced p-Akt activation by $PI3K^{DN}$ expression demonstrates that PI3K activity is required for this activation, it remains possible that glutamate increases p-Akt levels by activating an enzyme in addition to PI3K. For example, Akt is reported to be phosphorylated and activated by Calmodulin-dependent kinase kinase[50]. Further experiments will be required to address these issues.

Methods

Drosophila Stocks: Fly stocks were maintained on standard cornmeal/ agar Drosophila media at room temperature. *D42* and *OK6* express *Gal4* in motor neurons and were provided by Tom Schwarz, Boston, Massachusetts, and Hermann Aberle, Tubingen, Germany respectively. The *UAS-*$PI3K^{DN}$ (D954A) and *UAS-PI3K-CAAX* transgenes were provided by Sally Leevers, London, UK, the *UAS-*$Foxo^{+}$ transgene was provided by Marc Tatar, Providence, RI, the $Foxo^{21}$ and $Foxo^{25}$ lines were provided by Heinrich Jasper, Rochester, NY, the *UAS-*$S6K^{DN}$ and *UAS-*$S6K^{act}$ transgenes were provided by Ping Shen, Athens, GA, and the *UAS-*$mGluRA^{RNAi}$ and the $mGluRA^{112b}$ lines were provided by Marie-Laure Parmentier, Montpelier, France. All other fly stocks were provided by the Drosophila stock center, Bloomington, IN.

Immunocytochemistry: FITC conjugated antibodies against horseradish peroxidase (HRP) were raised in goat (Jackson ImmunoResearch) and were used at 1:400 dilution. Antibodies against Drosophila p-Akt (Ser505) were raised in rabbit (Cell Signaling Technologies) and were used at 1:500 dilution. Rhodamine Red conjugated goat anti-rabbit (Jackson ImmunoResearch) was used at a dilution of 1:1000. For arborization measurements, larvae were dissected in PBS-T and fixed in 4% paraformaldehyde. Images were taken on a Zeiss 410 laser scanning confocal microscope (LSM) with a 20x objective. ImageJ was used to obtain surface area measurements of muscle 6 from abdominal segment A3, and the number of boutons was counted manually. For p-Akt measurements, larvae were dissected in Grace's insect cell culture media (Gibco). When glutamate was applied,100 µM glutamic acid monosodium salt monohydrate (Acros Organics) dissolved in Grace's insect cell culture media was added to the well of the dissection plate. 1 minute after glutamate addition, larvae were rapidly washed in standard saline (0.128 M NaCl, 2.0 mM KCl, 4.0 mM $MgCl_2$, 0.34 M sucrose, 5.0 mM HEPES, pH 7.1, and 0.15 mM $CaCl_2$), and then immediately fixed in 4% paraformaldehyde. For the 10 min wash, the larvae were washed in Grace's insect cell culture media and placed on shaker for 10 minutes before fixing. Images were taken on a Zeiss 510 LSM with a 20x objective. Z-stacks were compiled from 2 µm serial sections to a depth adequate to encompass the entire bouton thickness for each sample (from 8-20 µm). Muscles 7 and 6 from either abdominal segments A3 or A4 were used for measurements. ImageJ software was used to analyze p-Akt intensities. In particular, 2D projections were created using the median pixel intensity from each stack at each coordinate point. Neuronal structures, marked by anti-HRP, were traced using the

freehand selection tool and the selection was transferred to the anti-p-Akt image where the mean pixel intensity value was measured. Background was obtained with a selection box encompassing the non-neuronal area of muscles 6 and 7 in the particular abdominal segment, the mean pixel intensity was measured and subtracted from the mean p-Akt pixel intensity.

Electrophysiology: The *D42* motor neuron driver was used to express transgenes for all experiments, except that the *OK6* driver was used for experiments including $Foxo^{21}/Foxo^{25}$. *OK6* behaves indistinguishably from *D42* in these assays (not shown) and is located on a different chromosome from *Foxo,* which simplifies stock construction. Larvae were grown to the wandering third-instar stage in uncrowded bottles at room temperature and dissected as described (17, 18) in standard saline solution (128 mM NaCl, 2.0 mM KCl, 4.0 mM $MgCl_2$, 340 mM sucrose, 5.0 mM HEPES, pH 7.1, and $CaCl_2$ as specified in the text). Peripheral nerves were cut posterior to the ventral ganglion and were stimulated using a suction electrode. Muscle recordings were taken from muscle 6 in abdominal sections 3-5. Recording electrodes were pulled using a Flaming/Brown micropipette puller to a tip resistence of 10-40 MΩ and filled with 3M KCl.

Electron Microscopy: Larvae were grown to the wandering third-instar stage in uncrowded bottles at room temperature. Dissections and preparation for microscopy were performed as previously described (47). Axon diameter measurements were taken from the five largest axons from five different nerves from at least two different larvae.

Statistics: Data are mean ± SEM. P values are from students two tailed t-tests.

Acknowledgments: We are grateful to Richard Gomer for insightful experimental suggestions, Marie-Laure Parmentier, Sally Leevers, Marc Tatar, Tom Schwarz, Heinrich Jasper, Ping Shen, Herman Aberle and the Drosophila stock center at Bloomington, IN for flies, Ming Yang, Alec Marin and Jason Mishaw for technical assistance, and James McNew and Dan Wagner for comments on the manuscript. Funded by grant W81XWH-04-1-0272 from the Department of Defense Neurofibromatosis Research Program (to MS).

1. Davis, G. W. Homeostatic Control of Neural Activity: From Phenomenology to Molecular Design. Annu Rev Neurosci (2006).
2. Marder, E. & Prinz, A. A. Current compensation in neuronal homeostasis. Neuron 37, 2-4 (2003).
3. Pozzi, D. et al. Activity-dependent phosphorylation of Ser187 is required for SNAP-25-negative modulation of neuronal voltage-gated calcium channels. Proc Natl Acad Sci U S A 105, 323-8 (2008).
4. Desai, N. S., Rutherford, L. C. & Turrigiano, G. G. Plasticity in the intrinsic excitability of cortical pyramidal neurons. Nat Neurosci 2, 515-20 (1999).

5. Echegoyen, J., Neu, A., Graber, K. D. & Soltesz, I. Homeostatic plasticity studied using in vivo hippocampal activity-blockade: synaptic scaling, intrinsic plasticity and age-dependence. PLoS ONE 2, e700 (2007).

6. Gibson, J. R., Bartley, A. F. & Huber, K. M. Role for the subthreshold currents ILeak and IH in the homeostatic control of excitability in neocortical somatostatin-positive inhibitory neurons. J Neurophysiol 96, 420-32 (2006).

7. Chen, C. Y., Ling Eh, E. H., Horowitz, J. M. & Bonham, A. C. Synaptic transmission in nucleus tractus solitarius is depressed by Group II and III but not Group I presynaptic metabotropic glutamate receptors in rats. J Physiol 538, 773-86 (2002).

8. Kew, J. N., Ducarre, J. M., Pflimlin, M. C., Mutel, V. & Kemp, J. A. Activity-dependent presynaptic autoinhibition by group II metabotropic glutamate receptors at the perforant path inputs to the dentate gyrus and CA1. Neuropharmacology 40, 20-7 (2001).

9. Poisik, O. et al. Metabotropic glutamate receptor 2 modulates excitatory synaptic transmission in the rat globus pallidus. Neuropharmacology 49 Suppl 1, 57-69 (2005).

10. Scanziani, M., Salin, P. A., Vogt, K. E., Malenka, R. C. & Nicoll, R. A. Use-dependent increases in glutamate concentration activate presynaptic metabotropic glutamate receptors. Nature 385, 630-4 (1997).

11. Schoepp, D. D. Unveiling the functions of presynaptic metabotropic glutamate receptors in the central nervous system. J Pharmacol Exp Ther 299, 12-20 (2001).

12. Patil, S. T. et al. Activation of mGlu2/3 receptors as a new approach to treat schizophrenia: a randomized Phase 2 clinical trial. Nat Med 13, 1102-7 (2007).
13. Swanson, C. J. et al. Metabotropic glutamate receptors as novel targets for anxiety and stress disorders. Nat Rev Drug Discov 4, 131-44 (2005).
14. Alexander, G. M. & Godwin, D. W. Metabotropic glutamate receptors as a strategic target for the treatment of epilepsy. Epilepsy Res 71, 1-22 (2006).
15. Anwyl, R. Metabotropic glutamate receptors: electrophysiological properties and role in plasticity. Brain Res Brain Res Rev 29, 83-120 (1999).
16. Bogdanik, L. et al. The Drosophila metabotropic glutamate receptor DmGluRA regulates activity-dependent synaptic facilitation and fine synaptic morphology. J Neurosci 24, 9105-16 (2004).
17. Jan, Y. N. & Jan, L. Y. Genetic dissection of short-term and long-term facilitation at the Drosophila neuromuscular junction. Proc Natl Acad Sci U S A 75, 515-9 (1978).
18. Stern, M. & Ganetzky, B. Altered synaptic transmission in Drosophila hyperkinetic mutants. J Neurogenet 5, 215-28 (1989).
19. Stern, M., Kreber, R. & Ganetzky, B. Dosage effects of a Drosophila sodium channel gene on behavior and axonal excitability. Genetics 124, 133-43 (1990).
20. Chouinard, S. W., Wilson, G. F., Schlimgen, A. K. & Ganetzky, B. A potassium channel beta subunit related to the aldo-keto reductase superfamily is encoded by the Drosophila hyperkinetic locus. Proc Natl Acad Sci U S A 92, 6763-7 (1995).
21. Loughney, K., Kreber, R. & Ganetzky, B. Molecular analysis of the para locus, a sodium channel gene in Drosophila. Cell 58, 1143-54 (1989).

22. Mallart, A., Angaut-Petit, D., Bourret-Poulain, C. & Ferrus, A. Nerve terminal excitability and neuromuscular transmission in T(X;Y)V7 and Shaker mutants of Drosophila melanogaster. J Neurogenet 7, 75-84 (1991).

23. Mee, C. J., Pym, E. C., Moffat, K. G. & Baines, R. A. Regulation of neuronal excitability through pumilio-dependent control of a sodium channel gene. J Neurosci 24, 8695-703 (2004).

24. Poulain, C., Ferrus, A. & Mallart, A. Modulation of type A K+ current in Drosophila larval muscle by internal Ca2+; effects of the overexpression of frequenin. Pflugers Arch 427, 71-9 (1994).

25. Schweers, B. A., Walters, K. J. & Stern, M. The Drosophila melanogaster translational repressor pumilio regulates neuronal excitability. Genetics 161, 1177-85 (2002).

26. Martin-Pena, A. et al. Age-independent synaptogenesis by phosphoinositide 3 kinase. J Neurosci 26, 10199-208 (2006).

27. Brand, A. H. & Perrimon, N. Targeted gene expression as a means of altering cell fates and generating dominant phenotypes. Development 118, 401-15 (1993).

28. Leevers, S. J., Weinkove, D., MacDougall, L. K., Hafen, E. & Waterfield, M. D. The Drosophila phosphoinositide 3-kinase Dp110 promotes cell growth. Embo J 15, 6584-94 (1996).

29. Ganetzky, B. & Wu, C. F. Drosophila mutants with opposing effects on nerve excitability: genetic and spatial interactions in repetitive firing. J Neurophysiol 47, 501-14 (1982).

30. Huang, Y. & Stern, M. In vivo properties of the Drosophila inebriated-encoded neurotransmitter transporter. J Neurosci 22, 1698-708 (2002).

31. Hay, N. & Sonenberg, N. Upstream and downstream of mTOR. Genes Dev 18, 1926-45 (2004).

32. Tang, E. D., Nunez, G., Barr, F. G. & Guan, K. L. Negative regulation of the forkhead transcription factor FKHR by Akt. J Biol Chem 274, 16741-6 (1999).

33. Cross, D. A., Alessi, D. R., Cohen, P., Andjelkovich, M. & Hemmings, B. A. Inhibition of glycogen synthase kinase-3 by insulin mediated by protein kinase B. Nature 378, 785-9 (1995).

34. Barcelo, H. & Stewart, M. J. Altering Drosophila S6 kinase activity is consistent with a role for S6 kinase in growth. Genesis 34, 83-5 (2002).

35. Junger, M. A. et al. The Drosophila forkhead transcription factor FOXO mediates the reduction in cell number associated with reduced insulin signaling. J Biol 2, 20 (2003).

36. Hwangbo, D. S., Gershman, B., Tu, M. P., Palmer, M. & Tatar, M. Drosophila dFOXO controls lifespan and regulates insulin signalling in brain and fat body. Nature 429, 562-6 (2004).

37. Vicario-Abejon, C., Owens, D., McKay, R. & Segal, M. Role of neurotrophins in central synapse formation and stabilization. Nat Rev Neurosci 3, 965-74 (2002).

38. Budnik, V., Zhong, Y. & Wu, C. F. Morphological plasticity of motor axons in Drosophila mutants with altered excitability. J Neurosci 10, 3754-68 (1990).

39. Broughton, S. J., Kitamoto, T. & Greenspan, R. J. Excitatory and inhibitory switches for courtship in the brain of Drosophila melanogaster. Curr Biol 14, 538-47 (2004).

40. Mosca, T. J., Carrillo, R. A., White, B. H. & Keshishian, H. Dissection of synaptic excitability phenotypes by using a dominant-negative Shaker K+ channel subunit. Proc Natl Acad Sci U S A 102, 3477-82 (2005).

41. Gorczyca, M., Augart, C. & Budnik, V. Insulin-like receptor and insulin-like peptide are localized at neuromuscular junctions in Drosophila. J Neurosci 13, 3692-704 (1993).

42. Shinoda, S. et al. Bim regulation may determine hippocampal vulnerability after injurious seizures and in temporal lobe epilepsy. J Clin Invest 113, 1059-68 (2004).

43. Kwon, C. H. et al. Pten regulates neuronal arborization and social interaction in mice. Neuron 50, 377-88 (2006).

44. Mills, J. L. et al. Elevated levels of growth-related hormones in autism and autism spectrum disorder. Clin Endocrinol (Oxf) 67, 230-7 (2007).

45. Dasgupta, B., Yi, Y., Chen, D. Y., Weber, J. D. & Gutmann, D. H. Proteomic analysis reveals hyperactivation of the mammalian target of rapamycin pathway in neurofibromatosis 1-associated human and mouse brain tumors. Cancer Res 65, 2755-60 (2005).

46. Johannessen, C. M. et al. The NF1 tumor suppressor critically regulates TSC2 and mTOR. Proc Natl Acad Sci U S A 102, 8573-8 (2005).

47. Lavery, W. et al. Phosphatidylinositol 3-kinase and Akt nonautonomously promote perineurial glial growth in Drosophila peripheral nerves. J Neurosci 27, 279-88 (2007).

48. Rong, R. et al. PI3 kinase enhancer-Homer complex couples mGluRI to PI3 kinase, preventing neuronal apoptosis. Nat Neurosci 6, 1153-61 (2003).

49. Diagana, T. T. et al. Mutation of Drosophila homer disrupts control of locomotor activity and behavioral plasticity. J Neurosci 22, 428-36 (2002).

50. Yano, S., Tokumitsu, H. & Soderling, T. R. Calcium promotes cell survival through CaM-K kinase activation of the protein-kinase-B pathway. Nature 396, 584-7 (1998).

Figure Legends

Figure 1. PI3K activity inhibits neuronal excitability by inhibiting the transcription factor Foxo. The motor neuron GAL4 driver *D42* was used to drive expression of all transgenes. For all LTF experiments, the bath solution contained 0.15 mM [Ca^{2+}] and 100 μM quinidine, which is a K^+ channel blocker that sensitizes the motor neuron and enables LTF to occur and measured even in hypoexcitable neurons. *A*, Representative traces showing the decreased rate of onset of long-term facilitation (LTF) (I) and decreased excitatory junction potential (ejp) amplitude (II) in larvae overexpressing *PI3K-CAAX* in motor neurons compared to wildtype at the indicated [Ca^{2+}], and the increased rate of onset of LTF and ejp amplitude in larvae overexpressing *PTEN*.

Arrowheads indicate the increased and asynchronous ejps, indicative of onset of LTF. In (II), ejps are averages of 180 responses for each genotype. *B, D* Number of stimulations required to induce LTF (Y axis) at the indicated stimulus frequencies (X axis) in the indicated genotypes. Geometric means +/- SEMs are shown. For B, from top to bottom, *n* = 8, 12, 18, 9, and 21, respectively, for each genotype. For D, from top to bottom, *n* = 7, 6, 18, 14, 9, and 7, respectively, for each genotype. *C,* Mean ejp amplitudes (Y axis) at the indicated [Ca^{2+}] (X axis), from the indicated genotypes. Larval nerves were stimulated at a frequency of 1 Hz, and 10 responses were measured from each of six larvae. Means +/- SEMs are shown.

Figure 2. A model for the negative feedback loop regulating motor neuron excitability. The transcription factor Foxo increases neuronal excitability through a mechanism possibly involving transcription of ion channel subunits or regulators. This increased excitability promotes glutamate release from motor nerve terminals, which then activates presynaptic DmGluRA in an autocrine manner. This activation, in turn, activates PI3K and the subsequent inactivation of Foxo by Akt-mediated inhibitory phosphorylation. Activated PI3K also promotes axonal growth and synapse formation via the Tor/S6K pathway.

Figure 3. A *Foxo - PI3K - DmGluR* epistasis series in the control of motor neuron excitability. The *Gal4* driver *D42* was used to drive expression of transgenes in all genotypes except for $Foxo^{21}/Foxo^{25}$; *OK6>*$PI3K^{DN}$, in which the motor neuron driver *OK6* was used and which behaves similarly to *D42* in this assay (not shown). A, Mean

ejp amplitude +/- SEMs (Y axis) for each genotype at the indicated [Ca^{2+}]. Nerves from six larvae were stimulated at a frequency of 1 Hz, and 10 responses were measured per larva. *B,* Number of stimulations required to induce LTF (Y axis) at the indicated stimulus frequencies (X axis). The bath solution contained 0.15 mM [Ca^{2+}] and 0.1 mM quinidine. Geometric means +/- SEMs are shown. From *top* to *bottom, n* = 7, 18, and 10, respectively, for each genotype.

Figure 4. Glutamate application stimulates presynaptic Akt phosphorylation in $DmGluRA^{+}$ but not in $DmGluRA^{112b}$ mutant larvae. *A,* Representative confocal images of in $DmGluRA^{+}$, $DmGluRA^{112b}$, $D42>mGluRA^{RNAi}$ and $D42>PI3K^{DN}$ larvae stained with anti-HRP (upper) and anti-p-Akt (lower) in the indicated conditions. All images are from muscles 7 and 6 of abdominal segment A3 or A4. Scale bar = 20 µm. *B,* Quantification of phosphorylated Akt (p-Akt) levels in $DmGluRA^{+}$, $DmGluRA^{112b}$, $D42>mGluRA^{RNAi}$ and $D42>PI3K^{DN}$ larvae immediately prior to glutamate application, after 1 min of 100 µM glutamate application (final bath concentration), and 10 min after a wash with glutamate free media. Nerve terminals were outlined with HRP fluorescence as reference. Pixel intensities were quantified using ImageJ software and background subtraction was performed as described in detail in Methods section. Bars represent mean synaptic p-Akt levels +/- SEMs. *D42 > PI3K-CAAX* is included as a positive control.

Figure 5. $PI3K^{DN}$ expression suppresses the synaptic overgrowth conferred by motor neuron expression of eag^{DN} and Sh^{DN}. The *D42 Gal4* driver was used to induce motor

neuron transgene expression. *A,* Representative confocal images of muscles 7 and 6 in the indicated genotypes. Larvae were stained with anti-HRP (green). Scale bar = 20 μm. *B,* Mean number of synaptic boutons normalized to the surface area (Y axis) of muscle 6 at abdominal segment A3 in the indicated genotypes (X axis). From *top* to *bottom*, *n* = 12, 6, 6 and 6 respectively, for each genotype.

Supplementary Information

Supplementary Figure 1: Effects of altered PI3K pathway activity on failures of transmitter release. *A,B* Mean transmitter release success rate +/- SEMs (Y axis) at the indicated Ca^{2+} concentration (X axis) for the indicated genotypes. Larval nerves were stimulated at 1 Hz. 10 responses were collected per nerve from each of 6 larvae for the given genotype and at the given Ca^{2+} concentration.

Supplementary Figure 2. PI3K regulates synapse formation and axon growth via S6K, not Foxo. *A,* Representative images of muscles 7 and 6 in the indicated genotypes. Larva were stained with anti-HRP (green). Scale bar = 50 μm. *B,* Quantification of the number of synaptic boutons normalized to the surface area of muscle 6 at abdominal segment A3 in the indicated genotypes. From left to right, n=6,8,6,6,7,6,11, respectively, for each genotype. Data for *D42>PI3K*^{DN} and *D42>+* were taken from Figure 5. *C,* Representative transmission electron micrographs of peripheral nerve cross sections.

Axons are marked with arrows. Scale bar = 2 μm. *D,* Quantification of axon diameter for the indicated genotypes. Bars represent the mean of the five largest axons from five different nerves (25 measurements total). Error Bars represent SEMs.

Supplementary Figure 3. A *Foxo - PI3K - DmGluR* epistasis series in the control of motor neuron excitability. The *Gal4* driver *D42* was used to drive expression of transgenes in all genotypes except for $Foxo^{21}/Foxo^{25}$; $OK6>PI3K^{DN}$, in which the motor neuron driver *OK6* was used and which behaves similarly to *D42* in this assay (not shown). Some of these data were reported in Figure 3 (indicated by hatched lines) and are shown here to enable comparisons with additional genotypes. A, Mean ejp amplitude +/- SEMs (Y axis) for each genotype at the indicated $[Ca^{2+}]$. Nerves from six larvae were stimulated at a frequency of 1 Hz, and 10 responses were measured per larva. *B*, Number of stimulations required to induce LTF (Y axis) at the indicated stimulus frequencies (X axis). The bath solution contained 0.15 mM $[Ca^{2+}]$ and 0.1 mM quinidine. Geometric means +/- SEMs are shown. From *top* to *bottom*, *n* = 7, 7, 18, 6, 10, and 8, respectively, for each genotype.

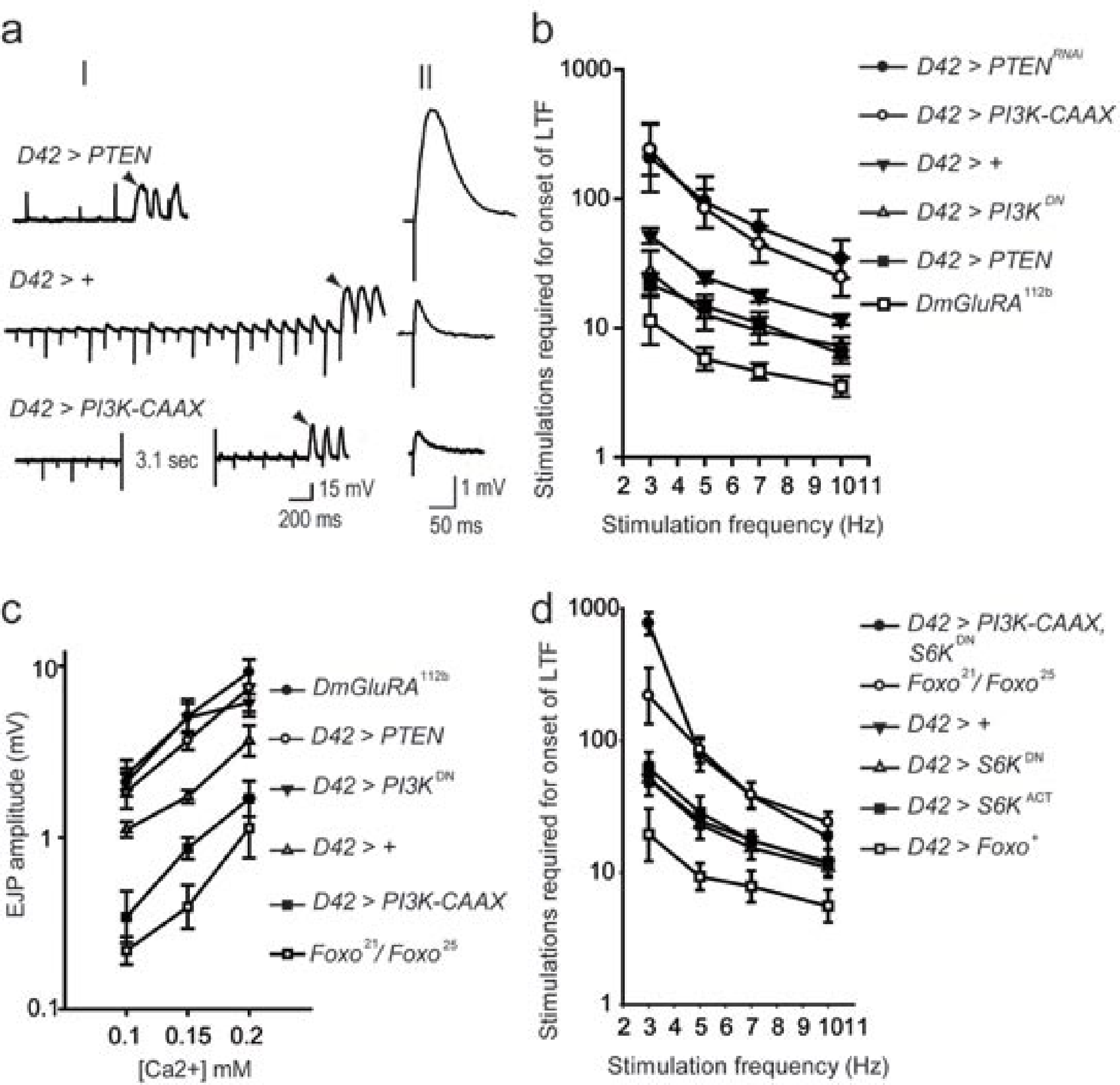
a
I
II
D42 > PTEN
D42 > +
D42 > PI3K-CAAX
3.1 sec
15 mV
200 ms
1 mV
50 ms
b
Stimulations required for onset of LTF
1000
100
10
1
2 3 4 5 6 7 8 9 10 11
Stimulation frequency (Hz)
D42 > PTEN^RNAi
D42 > PI3K-CAAX
D42 > +
D42 > PI3K^DN
D42 > PTEN
DmGluRA^112b
c
EJP amplitude (mV)
10
1
0.1
0.1 0.15 0.2
[Ca2+] mM
DmGluRA^112b
D42 > PTEN
D42 > PI3K^DN
D42 > +
D42 > PI3K-CAAX
Foxo^21/ Foxo^25
d
Stimulations required for onset of LTF
1000
100
10
1
2 3 4 5 6 7 8 9 10 11
Stimulation frequency (Hz)
D42 > PI3K-CAAX, S6K^DN
Foxo^21/ Foxo^25
D42 > +
D42 > S6K^DN
D42 > S6K^ACT
D42 > Foxo*

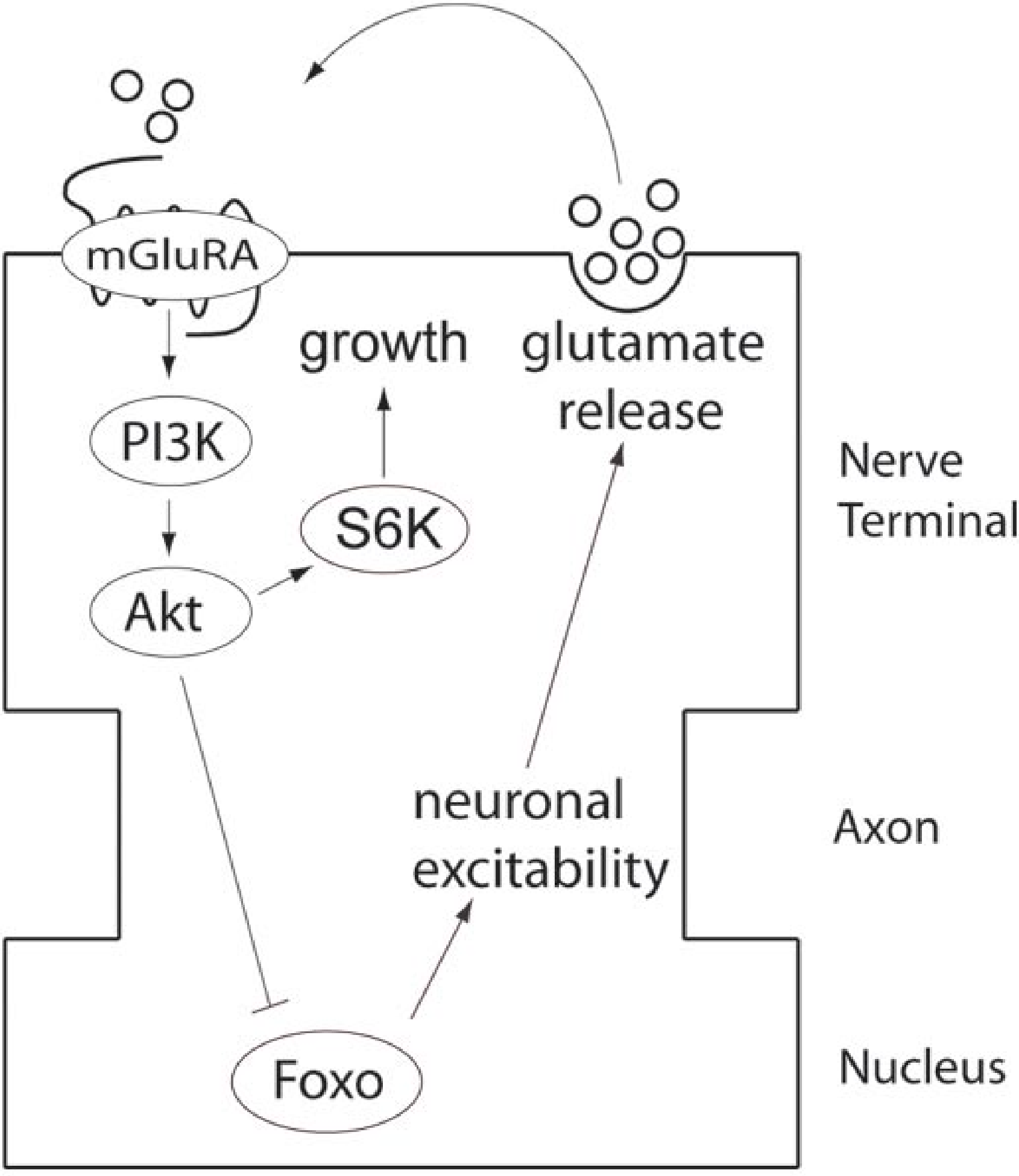
mGluRA
growth
glutamate
release
PI3K
S6K
Akt
Nerve
Terminal
neuronal
excitability
Axon
Foxo
Nucleus

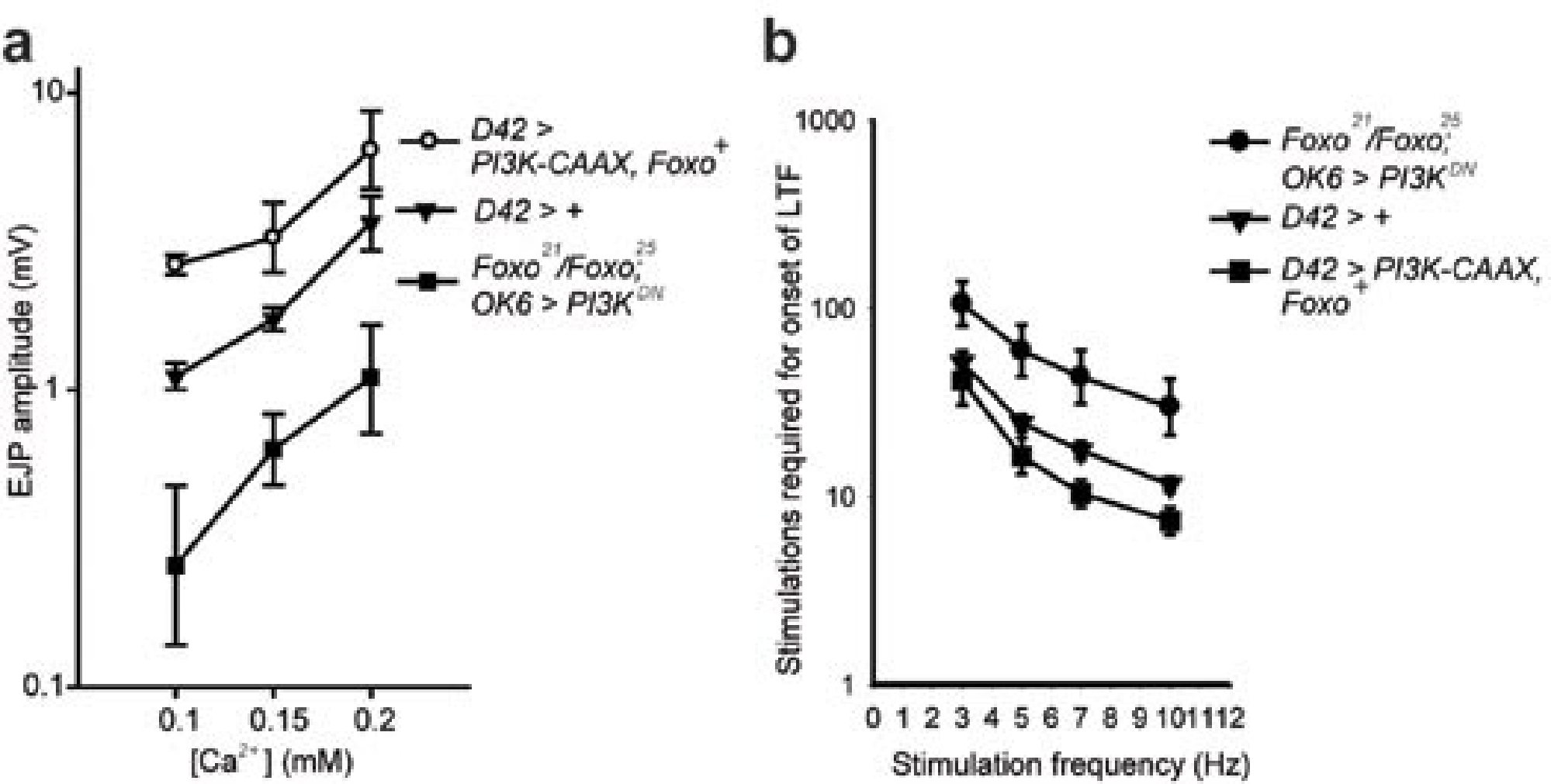
a
10
1
0.1
EJP amplitude (mV)
0.1
0.15
0.2
[Ca2+] (mM)
D42 > PI3K-CAAX, Foxo+
D42 > +
Foxo21/Foxo25; OK6 > PI3KDN
b
1000
100
10
1
Stimulations required for onset of LTF
0 1 2 3 4 5 6 7 8 9 10 11 12
Stimulation frequency (Hz)
Foxo21/Foxo25; OK6 > PI3KDN
D42 > +
D42 > PI3K-CAAX, Foxo+

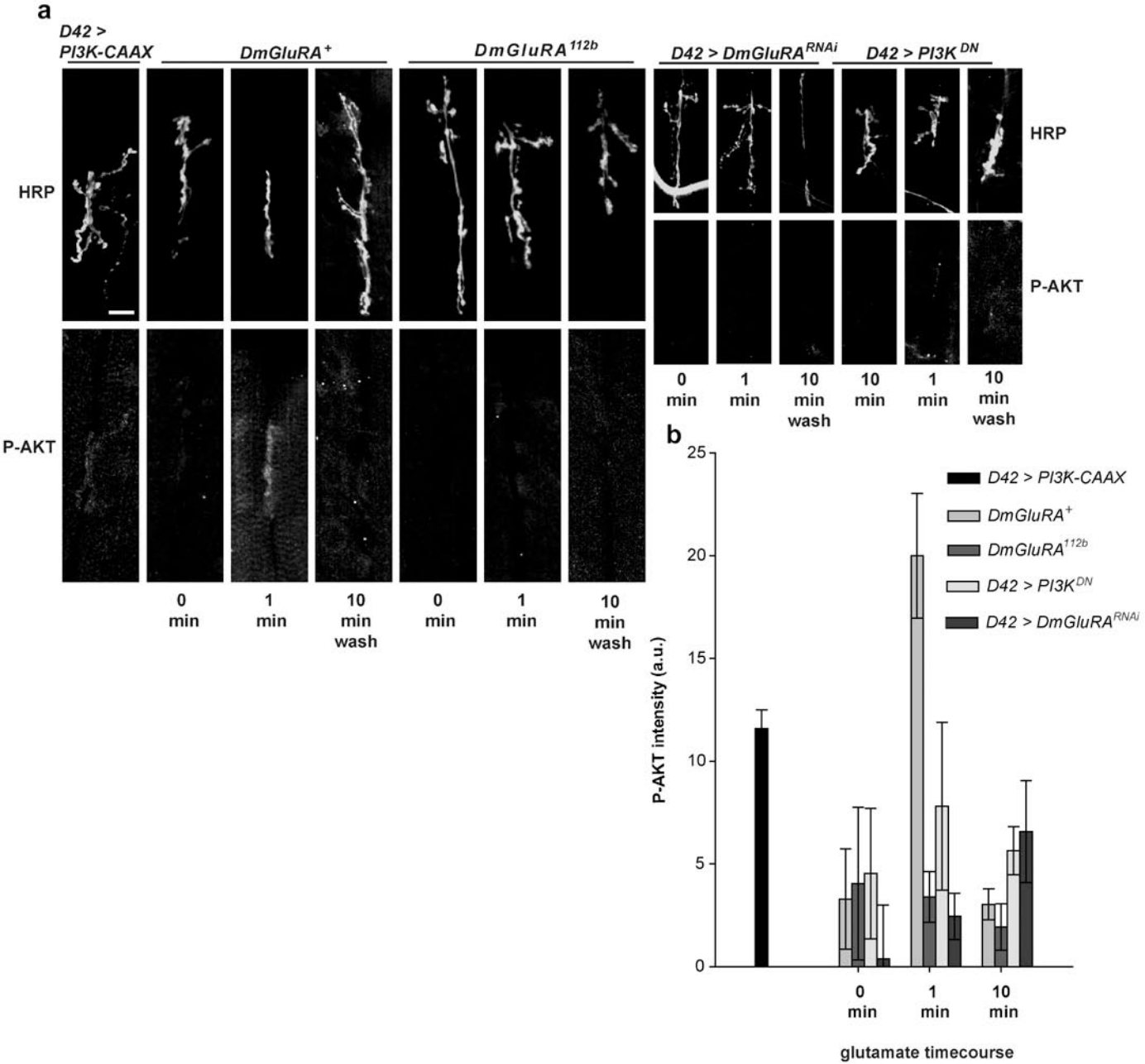
a
D42 > PI3K-CAAX
DmGluRA+
DmGluRA112b
D42 > DmGluRARNAi
D42 > PI3K DN
HRP
P-AKT
0 min
1 min
10 min wash
10 min
1 min
10 min wash
b
P-AKT intensity (a.u.)
glutamate timecourse
D42 > PI3K-CAAX
DmGluRA+
DmGluRA112b
D42 > PI3KDN
D42 > DmGluRARNAi

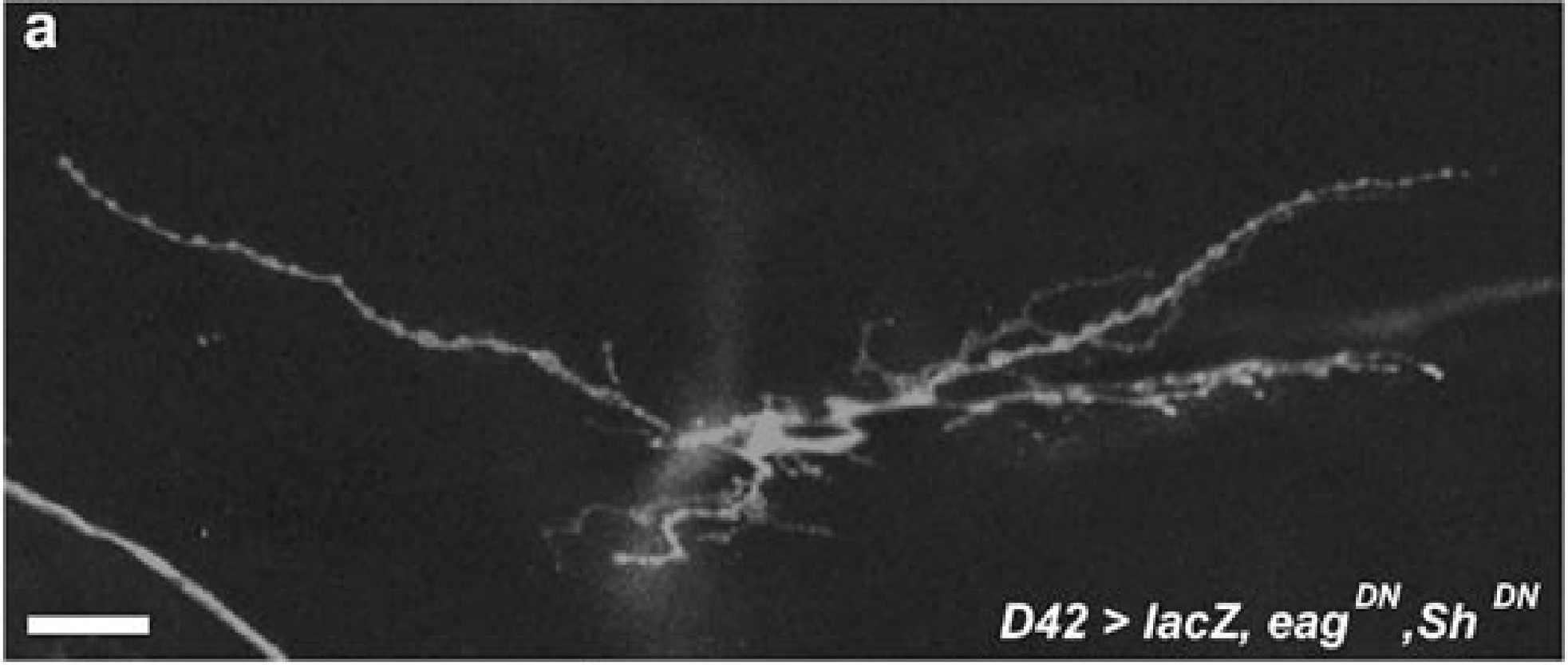
a
D42 > lacZ, eag DN ,Sh DN

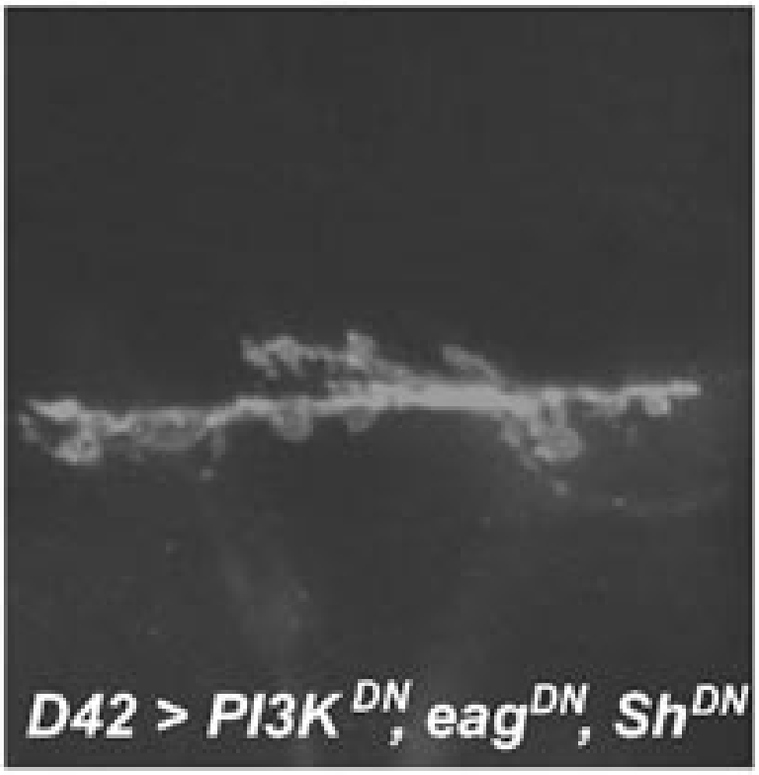
D42 > PI3K DN; eag DN, Sh DN

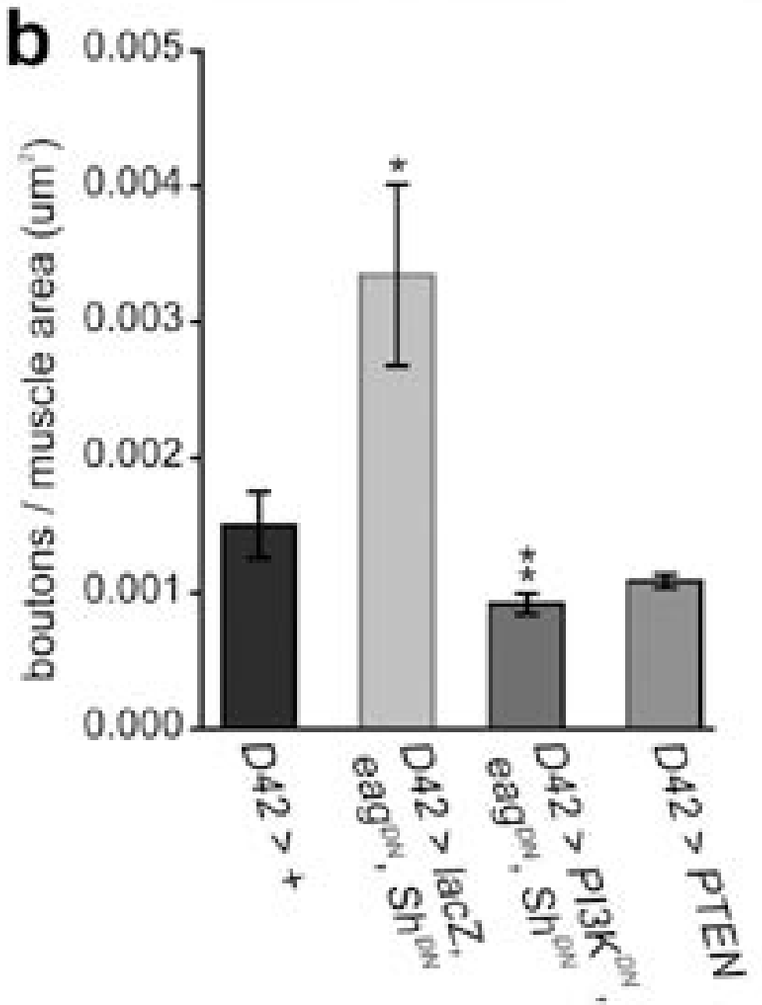
b
boutons / muscle area (um-2)
0.005
0.004
0.003
0.002
0.001
0.000
*
**
D42 > +
D42 > lacZ, eag DN, Sh DN
D42 > PI3K DN, eag DN, Sh DN
D42 > PTEN

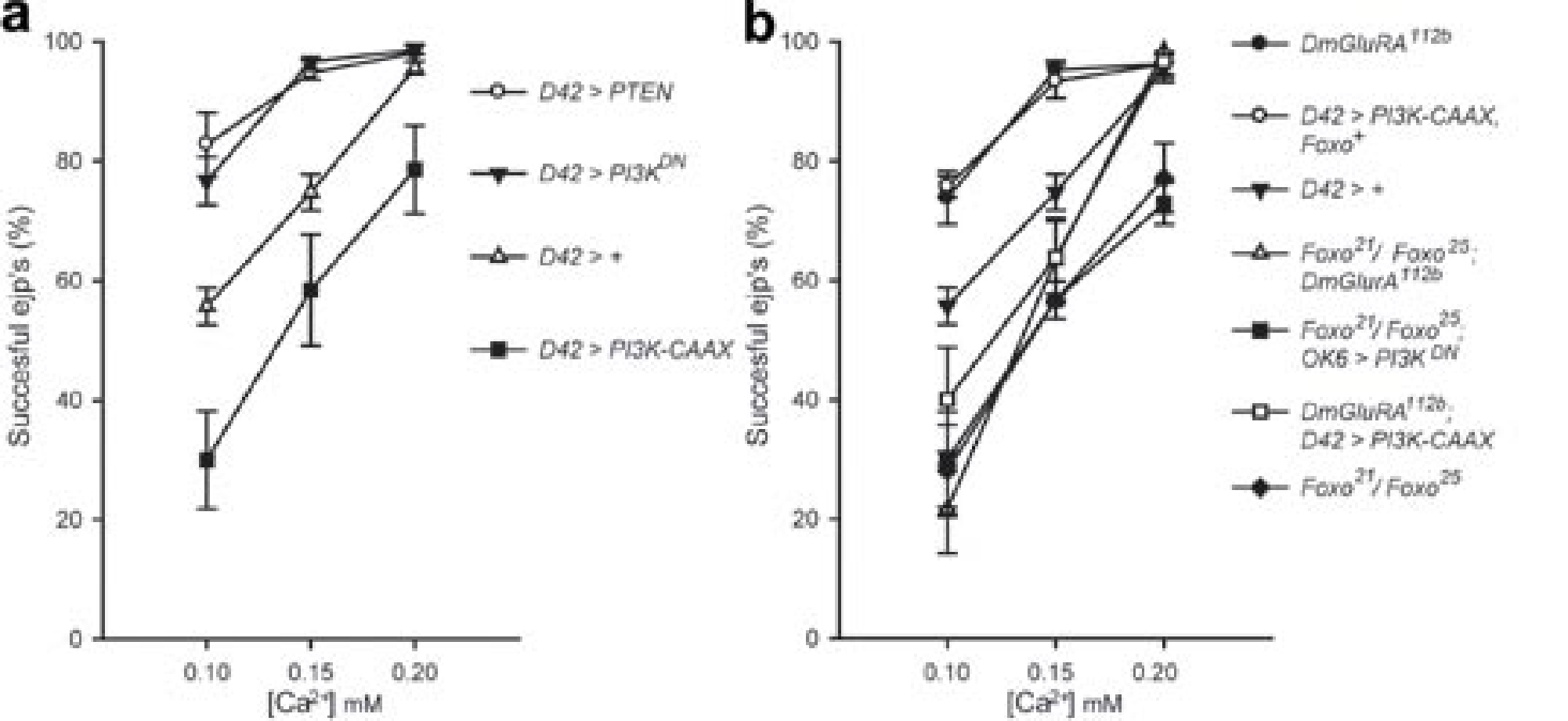
a
b
Succesful ejp's (%)
100
80
60
40
20
0
0.10
0.15
0.20
[Ca2+] mM
D42 > PTEN
D42 > PI3K^DN
D42 > +
D42 > PI3K-CAAX
DmGluRA^112b
D42 > PI3K-CAAX, Foxo+
D42 > +
Foxo^21/ Foxo^25; DmGluRA^112b
Foxo^21/ Foxo^25; OK6 > PI3K^DN
DmGluRA^112b; D42 > PI3K-CAAX
Foxo^21/ Foxo^25

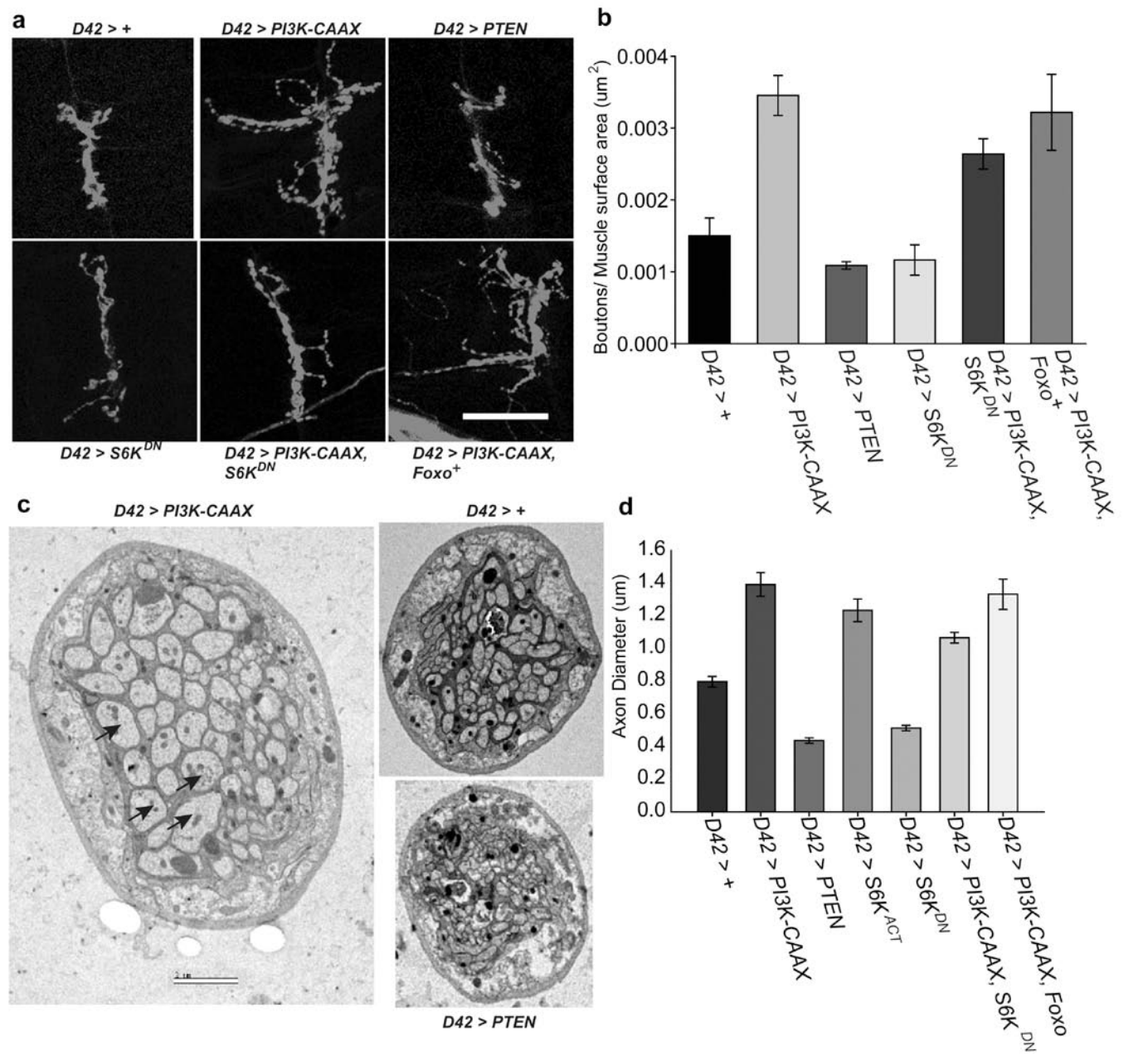
a
D42 > +
D42 > PI3K-CAAX
D42 > PTEN
D42 > S6K^DN
D42 > PI3K-CAAX, S6K^DN
D42 > PI3K-CAAX, Foxo+
b
Boutons/ Muscle surface area (um^2)
0.004
0.003
0.002
0.001
0.000
D42 > +
D42 > PI3K-CAAX
D42 > PTEN
D42 > S6K^DN
D42 > PI3K-CAAX, S6K^DN
D42 > PI3K-CAAX, Foxo+
c
D42 > PI3K-CAAX
D42 > +
D42 > PTEN
d
Axon Diameter (um)
1.6
1.4
1.2
1.0
0.8
0.6
0.4
0.2
0.0
D42 > +
D42 > PI3K-CAAX
D42 > PTEN
D42 > S6K^ACT
D42 > S6K^DN
D42 > PI3K-CAAX, S6K^DN
D42 > PI3K-CAAX, Foxo

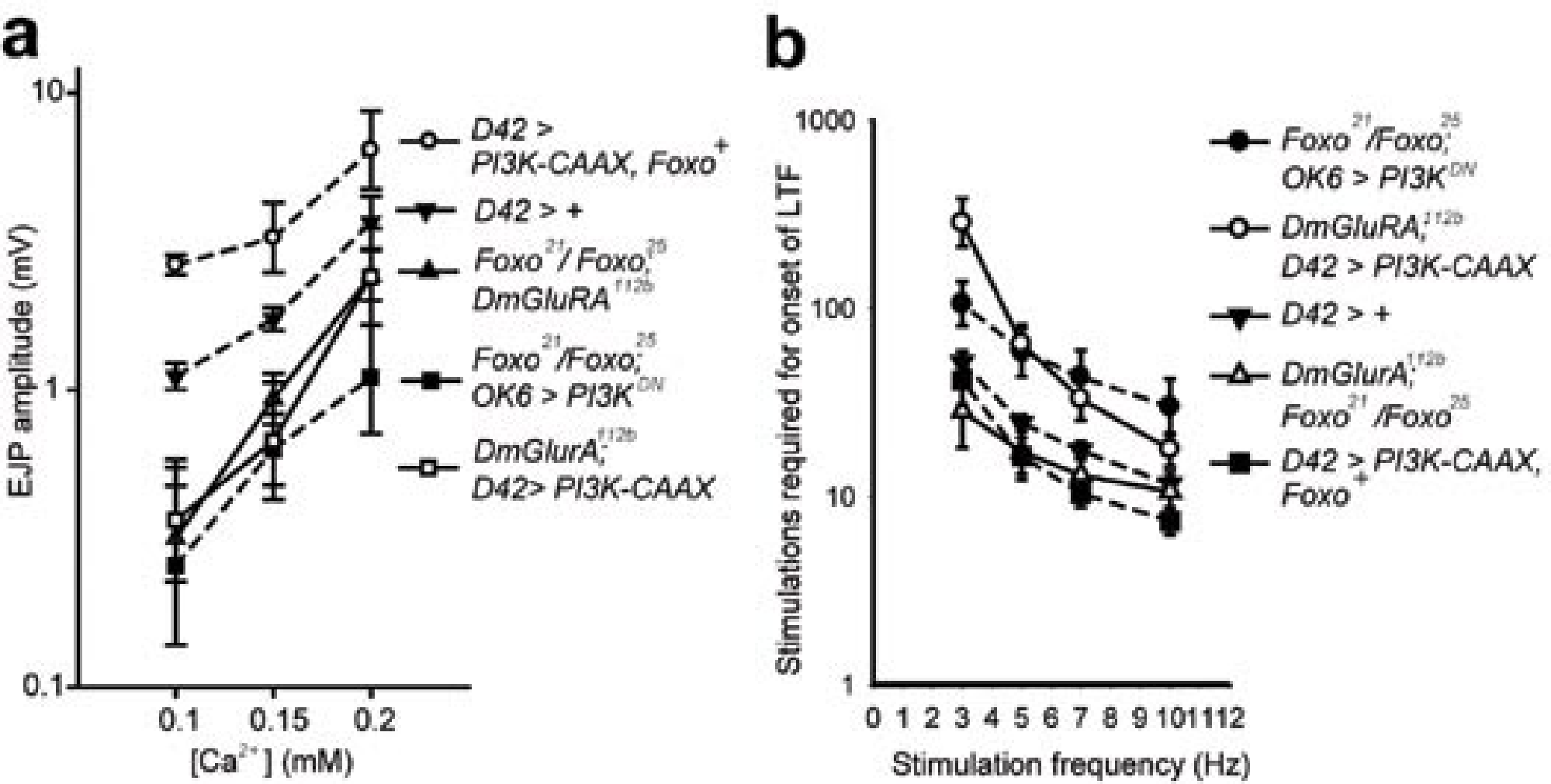
a
10
1
0.1
EJP amplitude (mV)
0.1
0.15
0.2
[Ca2+] (mM)
D42 > PI3K-CAAX, Foxo+
D42 > +
Foxo21 / Foxo25; DmGluRA112b
Foxo21 /Foxo25; OK6 > PI3KDN
DmGlurA112b; D42> PI3K-CAAX
b
1000
100
10
1
Stimulations required for onset of LTF
0 1 2 3 4 5 6 7 8 9 10 11 12
Stimulation frequency (Hz)
Foxo21 /Foxo25; OK6 > PI3KDN
DmGluRA112b; D42 > PI3K-CAAX
D42 > +
DmGlurA112b; Foxo21 /Foxo25
D42 > PI3K-CAAX, Foxo+